Effect of the electric field on magnetic properties of linear chains on a Pt(111) surface

T. R. Dasa, P. A. Ignatiev, and V. S. Stepanyuk*
Max-Planck-Institut für Mikrostrukturphysik, Weinberg 2, D-06120 Halle, Germany
(Received 10 January 2012; revised manuscript received 23 April 2012; published 25 May 2012)

Performing state-of-the-art *ab initio* calculations we study the effect of the electric field on magnetic properties of Co and Co-Pt chains on Pt(111). Our studies give clear evidence that an externally applied electric field could permit one to tailor magnetic anisotropy in chains. It is demonstrated that the physics behind this effect is related to the spin-dependent screening of an external electric field at the chains. A strong enhancement of magnetic anisotropy energy in mixed Co-Pt chains, compared to pure Co chains, is found. The interplay between atomic structure and the magnetic anisotropy energy is discussed.

DOI: 10.1103/PhysRevB.85.205447 PACS number(s): 73.22.−f, 71.15.Mb, 75.30.Gw, 75.75.−c

I. INTRODUCTION

Recent studies in the areas of magnetoelectronics and spintronics suggest that it could be worthwhile to control magnetic properties of devices and their elements by means of the electric field.[1–3] The coupling between electric and magnetic properties of a material, i.e., the magnetoelectric effect, has already been suggested as a new promising technology for magnetic data storage devices.[4,5] There are two mainstream approaches to exploit magnetoelectric phenomena in device applications. The first one is based on multiferroic, multifunctional materials, where the coupling between the magnetic properties and the external electric field is provided by the change of the structure due to the field-induced polarization.[6–9] A field effect transistor based on a single-phase $BiFeO_3$ multiferroic has been recently created.[10,11] Another way to couple the electric field and magnetic properties is implemented in magnetic semiconductors with carrier-mediated magnetic interaction. The applied field alters the concentration of carriers, thus varying the magnetic interaction and, consequently, the magnetic order. This scheme was implemented in experimental devices based on Mn-doped InAs.[9] The gate voltage controls the concentration of holes mediating the interaction between Mn dopants. Unfortunately, both of the approaches mentioned have a major drawback: The critical temperature, at which thermal fluctuations destroy magnetic order, is too low for most semiconductors and multiferroics.[12] Only very recently a magnetic semiconductor, which allows switching its magnetic state from the paramagnetic to the ferromagnetic one at room temperature by means of the gate voltage, has been invented.[13]

The problem of thermal instability can be solved by using Pd/Pt-3dM compounds, which have blocking temperature T_b far above the room temperature.[14] The high T_b of these compounds is explained by the large magnetic anisotropy. Achieving a giant magnetic anisotropy energy (MAE) is, thus, of crucial importance and could be used to stabilize magnetic moments against thermal fluctuations. MAE can be enhanced if magnetic nanomaterials of reduced dimensions are used. For example, it was shown that 0D (adatoms)[15,16] and 1D (chains and wires)[17–23] nanostructures on metal surfaces exhibit larger MAE than bulk structures. The experimental study of Co clusters supported by the Pt(111) surface showed that the MAE per Co atom increases while the cluster size decreases; indeed, for a single Co adatom a giant MAE of 9 meV was measured.[15,24,25] Large MAE of Co chains on the Pt(997) surface was observed.[21] Nowadays, clusters and chains of various sizes and compositions can be created on surfaces by means of STM manipulation.[26–31] The alternative way is to evolve nanostructures using atomic self-assembly.[32–35] A reduced dimensionality of Pt-3dM nanochains and a large spin-orbit coupling of Pt may lead to a large MAE.

The MAE can be tuned by the electric field.[14,36,37] For example, it has been revealed that the net charge of Fe-Pt/Pd films embedded in an electrolyte medium is changed upon exposure to the external electric field.[14] The corresponding variation in the number of unpaired d electrons in the response to the applied electric field changes the MAE. In the Fe/MgO tunneling junction, a large change in MAE has been observed when the external electric field was applied.[36] This phenomenon originates from the change in the electron filling of the Fe layer. Other experimental studies on magnetic nanostructures and junctions show that it is also possible to modify magnetic properties using an electric field.[38–41] The magnetoelectric effect on surfaces, thin films, and atomic chains has been confirmed by theoretical studies.[42–49,51] As an example, Fe monolayers on the Pt(001) and Pd(001) surfaces exhibit a linear dependence of MAE on the applied electric field, and it was revealed that the relative increase of MAE was higher in Pt than in Pd substrate by a significant factor.[44,45] Similar works on monolayers and thin films confirm such an effect.[46] The electric field has been used to switch the magnetic states of Mn dimers on metal surfaces.[47] In another study,[50] it was found that the MAE of freestanding Fe chains could be altered by the external electric field.

In the present work we concentrate on the effect of the electric field on magnetic properties of atomic chains on metal surfaces. As a model system we choose pure Co and mixed Co-Pt chains on the Pt(111) surface. In fact such systems could be produced at low temperatures using STM.[29] We reveal the interplay between atomic relaxations (in the chain and the substrate) and the MAE. Our studies demonstrate that the MAE in Co-Pt chains on the Pt(111) surface is enhanced by 35% compared to the MAE of pure Co chains. We have found that atomic relaxations in Co-Pt chains and the Co chain increase the MAE. Varying an external electric field from -1 V/Å to 1 V/Å, one can significantly increase or decrease the MAE (by 67%). The organization of the paper is the following:

Computational aspects of the work are covered in Sec. II. Our results related to the interplay between structural effects and magnetic properties and to the effect of the electric field on MAE are presented in Sec. III and Sec. IV, respectively. Finally, a brief conclusion is presented in Sec. V.

II. COMPUTATIONAL METHOD

The calculations were performed in the framework of the density functional theory using the projector augmented wave technique[53,54] implemented in the VASP code.[55,56] The exchange correlation effects were treated using the local spin density approximation (LSDA) by Cerperly and Adler.[57] The general gradient approximation (GGA, PBE)[58] was also used for test calculations. The spin-orbit coupling (SOC) was included self-consistently. The MAE was calculated from the ground state energies for magnetization aligned in the most relevant directions. A charge density cutoff of 400 eV was used for the plane wave expansion, and the ground state energies were converged down to the difference of 10^{-6} eV. To calculate the MAE, which is of the order of meV, the use of dense k-point meshes is compulsory. We used $4 \times 16 \times 1$ and $4 \times 8 \times 1$ k-point samplings of the Brillouin zone for the Co chain and the mixed Co-Pt chain on the Pt(111) surface, respectively.[61] A smearing parameter of 2 meV was applied.

The systems that we consider are the pure Co chain and the mixed Co-Pt chain on the Pt(111) substrate. The mixed Co-Pt linear chain is a 50% composition of each Co and Pt atoms on the Pt(111) surface. The top view of the unit cells is shown in Fig. 1(a) and 1(b), for the Co chain and the Co-Pt chain, respectively. The lattice constant of bulk Pt (3.91 Å), using LDA, was optimized using the Birch-Murnaghan equation of states.[59] Surface slabs were built using six layers of Pt atoms stacked in the (111) manner based on the bulk lattice parameter. We used 4×1 and 4×2 supercells for the Co chain and the Co-Pt chains, respectively. The nanochains are located on one side of the Pt slab. The system was relaxed until the forces acting on each atom were less than 5 meV/Å. The magnetization direction ($\vec{M}$) was defined using polar angles θ and ϕ. Angles θ and ϕ use the z axis and x axis, respectively, as reference Cartesian axes; this is shown in Fig. 1(c). A static electric field was applied perpendicular to the surface and dipole correction was taken into account.[60] A positive electric field is directed towards the side of the slab which holds the atomic chains, and vice versa for a negative electric field.

III. RESULTS AND DISCUSSION

A. Effect of structural relaxations on magnetic properties

In this section we discuss structural and magnetic properties of the Co and the Co-Pt chains on the Pt(111) surface. In Fig. 2 we present the relaxed geometry of both chains. The bond length and the vertical distances to the substrate are shown. The nanochains were initially placed at the height of the bulk interlayer distance of 2.25 Å, with respect to the topmost layer of the Pt(111) surface. Starting from the ideal geometry, we relaxed the structure by minimizing the forces. In the relaxed geometry of the Co chain on the Pt(111) surface, the Co atom lies at the distance of 1.71 Å from the surface and its magnetic

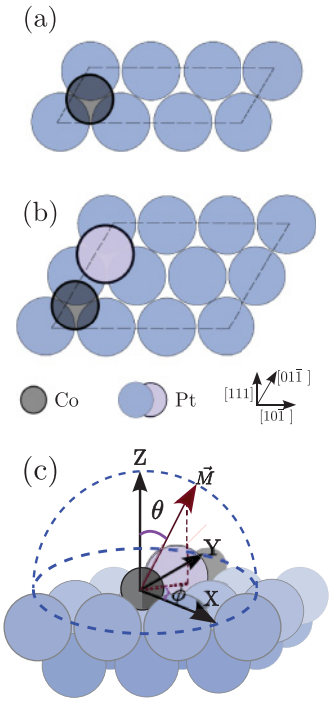

FIG. 1. (Color online) Schematics for the unit cells of (a) pure Co chains and (b) mixed Co-Pt chains on Pt(111) surface. (c) A sketch of the Cartesian and polar frames, used for the definition of the magnetization ($\vec{M}$). Angles θ and ϕ are measured with respect to z axis and x axis. Pt atoms in the chain and the substrate are represented by dark edge ring and light edge rings, respectively. The atomic chains on the surface are constructed in the [10$\bar{1}$] crystallographic direction of Pt(111).

properties are changed. Our results are reported in Table I for both relaxed and nonrelaxed geometries of Co chains.

First, we concentrate on the Co chains on the Pt(111) surface. The easy axis of the Co chain in the nonrelaxed geometry lies out of the surface plane ($\theta = 0^\circ$ and $\phi = 0^\circ$),

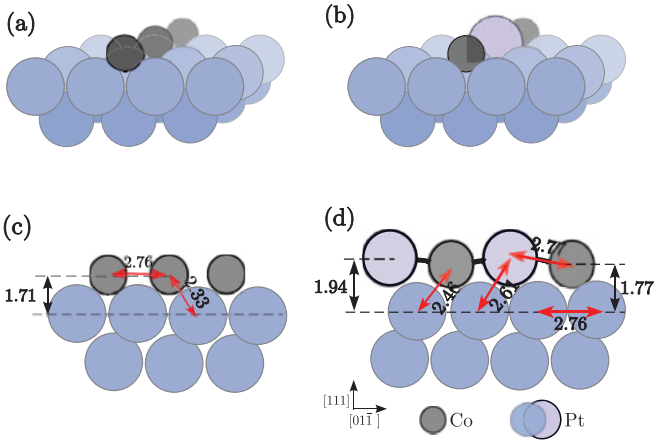

FIG. 2. (Color online) A sketch for the crystallographic structure of (a) the pure Co chain and (b) the mixed Co-Pt chain. The vertical distance between the atomic chains and the top layer are shown in (c) and (d). All the distances shown in the figure are in units of angstroms. The easy axes of relaxed structures of both systems are directed perpendicular to the surface ($\theta = 0$ and $\phi = 0$).

TABLE I. Spin magnetic moments (m_s), orbital magnetic moments (m_o), and the MAE of pure Co and the mixed Co-Pt chains in the Pt(111) surface. The two columns represent relaxed and unrelaxed geometries. Pt atoms in the mixed chain and Pt substrate atoms nearest to the chain are denoted by Pt_1 and Pt_2, respectively. All the spin magnetic moments are presented for the easy axis of magnetization.

	Pure Co Chain		Mixed Co-Pt Chain	
	Unrelaxed	Relaxed	Unrelaxed	Relaxed
MAE (meV)	2.2	2.8	2.0	4.3
Co, m_s (μ_B)	2.1	2.0	2.22	2.03
Co, m_o(easy) (μ_B)	0.29	0.16	0.29	0.19
Co, m_o(hard) (μ_B)	0.16	0.07	0.14	0.1
Pt_1, m_s (μ_B)			0.23	0.18
Pt_2, m_s (μ_B)	0.13	0.26	0.15	0.08
Easy axis (θ,ϕ)	(0,0)	(0,0)	(90,90)	(0,0)
Hard axis (θ,ϕ)	(90,0)	(90,0)	(90,0)	(90,0)

and the MAE is 2.2 meV.[61] When the system is relaxed the easy axis of magnetization is still oriented perpendicular to the surface, and the value of MAE is 2.8 meV. The spin and orbital moments of Co atoms in the chain, for the out-of-plane direction, change after relaxation from 2.1 μ_B to 2.0 μ_B, and from 0.29 μ_B to 0.16 μ_B, respectively. From Table I the higher value of the spin moment of the Pt substrate in the relaxed structure is explained by the shorter bond lengths [Fig. 2(c)], which provide a stronger hybridization between d states of Co and Pt. In our calculation, the Pt atoms in the substrate have an induced magnetic moment of 0.26 μ_B in relaxed geometry.

Similar noncollinear calculations were performed using the GGA (PBE)[58] exchange-correlation functional, for relaxed pure Co chains on the Pt(111) surface. The equilibrium lattice parameter is 3.99 Å. It was found that the MAE is 2.8 meV and the easy axis is oriented perpendicular to the surface. Compared to the LDA the spin magnetic moment of Co and Pt increases by 0.05 μ_B and 0.01 μ_B, respectively. At the same time, the orbital moment of Co atoms in the Co chain is reduced in the case of the GGA. To address recent calculations[52] performed for Co chains on Pt(111), we also did similar studies by means of the PWscf code of Quantum-ESPRESSO[64] using the LDA fully relativistic ultrasoft pseudopotential (USPP). Employing a lattice parameter of 3.92 Å, the MAE in the relaxed geometry was found to be 0.9 meV and the easy axis is in-plane along the direction of the chain (90, 90), which agrees with Ref. 52. However, with regard to both the MAE and the easy axis, these results do not agree with those based on the PAW technique. Further studies have been done using LDA, VASP to see the change of MAE with respect to the variation in the lattice parameter. At 4.08 Å we observe a decrease in the MAE (1.04 meV) and switch of the easy axis, from out of plane to in plane (along the chain). This leads to the conclusions that the MAE strongly depends on the lattice parameter. The origin of the discrepancy between the PAW and the USPP calculations is unclear for us. We believe that the PAW pseudopotential is more accurate than the ultrasoft pseudopotential.

We now discuss the Co-Pt atomic chains supported on the Pt(111) surface. The summary of the results on the interplay between magnetic properties and the geometrical relaxation of the Co-Pt mixed chain is presented in Table I. The vertical distance of the chain atoms from the surface and the length of the bonds are displayed in Fig. 2. The Co and Pt atoms in the chain are situated at the vertical distances of 1.77 Å and 1.94 Å from the Pt surface, respectively. The Co atom in the Co-Pt mixed chain lies 4% higher compared to the vertical distance of the Co atom in the relaxed Co chain. As a result of oscillatory vertical distance of Co and Pt atoms along the chain, the Co-Pt chain forms a zigzag-like shape. The interaction between the Co atom and the Pt atom is stronger than the interaction between Pt atoms, which is the reason for the stronger relaxation of the Co atom towards the Pt surface than the Pt atoms in the chain. In addition, the Co atoms in the Co-Pt chain also interact with Pt atoms in the chain, which prefer to stay higher.

The spin and orbital magnetic moments of the Co atom in the relaxed (nonrelaxed) geometries are 2.03 (2.22) μ_B and 0.19 (0.29) μ_B, respectively. In nonrelaxed geometry, the Pt atom in the chain has a spin magnetic moment of 0.23 μ_B. The induced magnetic moment of the Pt atom in the substrate is 0.15 μ_B. In the relaxed geometry the Pt atom in the chain and the Pt atom in the substrate have magnetic moments of 0.18 μ_B and 0.08 μ_B, respectively. For both relaxed and unrelaxed geometries the Pt atom in the chain has less coordination number than the one in the Pt(111) surface, which is the origin for the higher induced magnetic moments of Pt in the chain. The approximation which correlates MAE and orbital anisotropy, $\mathrm{MAE} = \varepsilon/4\mu_B[m_o(\mathrm{easy}) - m_o(\mathrm{hard})]$,[65–67] is valid for all systems and geometries that are considered in this study, where ε is the spin-orbit coupling constant. The MAE per atom is evaluated for isolated chains of Co and Co-Pt chains with respective interatomic distance of 2.76 Å and 2.77 Å, the distance between the atoms on the Pt(111) surface. A very high MAE is found to be 31 meV and 22 meV, with an easy axis perpendicular to the chain and parallel to the chain for Co and Co-Pt chains, respectively. The relation between MAE and orbital anisotropy is valid for the freestanding Co-Pt chain.

As shown in Table I, the MAE in the Co-Pt chain increases from 2.0 meV for a nonrelaxed geometry to 4.3 meV for the relaxed one.[62] The enhancement of the MAE due to atomic relaxations could be explained using the second-order perturbative consideration.[45,68] The energy difference between two quantization axes, the x axis and the z axis, can be written

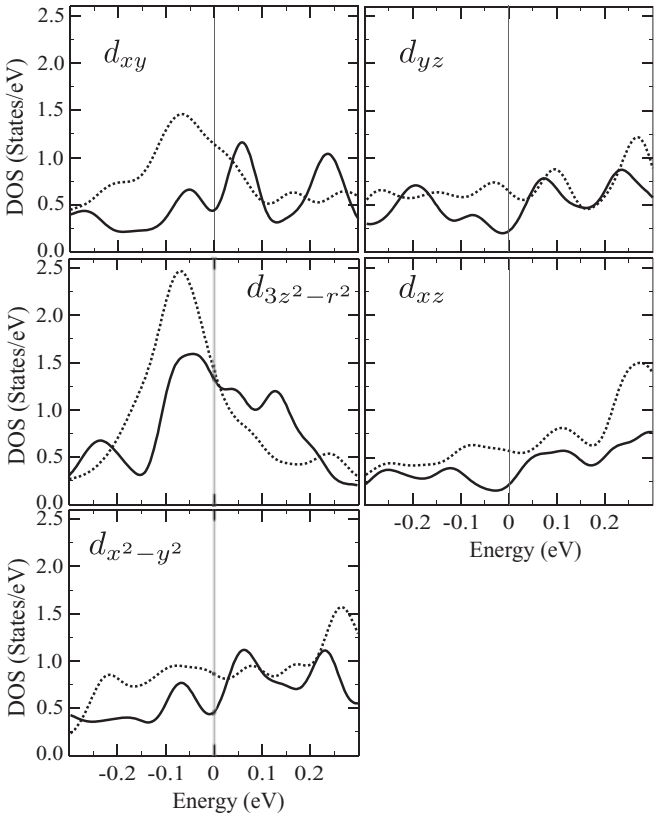

FIG. 3. Orbital-projected minority d LDOS of the Co atom in the Co-Pt chain (without external electric field), for relaxed (full lines) and unrelaxed (dashed lines), is represented. Only the minority density of states is considered, because the density of majority states is negligibly small at the Fermi level.

in simplified form as

$$\mathrm{MAE} \propto \sum_{kl} \frac{|\langle\phi_k|\vec{l}_z|\phi_l\rangle|^2 - |\langle\phi_k|\vec{l}_x|\phi_l\rangle|^2}{\varepsilon_k - \varepsilon_l}, \qquad (1)$$

where ϕ_l and ϕ_k are occupied and unoccupied states, and $\vec{l}_x$ and $\vec{l}_z$ are angular momentum operators. The second quantization contribution due to the spin-orbit coupling between occupied and unoccupied eigenstates near the Fermi level affects the ground state energy at most.[45,65,68] The orbital-projected LDOS for the minority d states of Co atom in the Co-Pt chain, which are the most dominant states near the Fermi energy, are shown in Fig. 3. Relaxations split the degenerate d levels in a close proximity to the Fermi energy providing, thus, the first contribution to the change of the MAE.

In the nonrelaxed Co-Pt chain the easy axis of magnetization is directed along the chain direction ($\phi = 90$ and $\theta = 90$) and the MAE is 2 meV. Following geometrical relaxation the easy axis changes to normal to the surface ($\phi = 0$ and $\theta = 0$) and the MAE increases by more than two times. In the nonrelaxed geometry there is a higher density of d_{xy} and $d_{3z^2-r^2}$ states just below the Fermi energy; however for relaxed geometry these states split and the density of states is shifted to higher energies (Fig. 3). The later effect, i.e., redistribution of d_{xy}, $d_{x^2-y^2}$, and $d_{3z^2-r^2}$ states around the Fermi energy, decreases the SOC between $d_{3z^2-r^2}$ states with d_{xz} and d_{yz} coupled by the $\vec{l}_x$ operator [Eq. (1)]. Additionally, from the change in the spin-orbit coupling matrix element for the easy and hard axis, which is provided in the VASP code,[69] the coupling between occupied and unoccupied states of d_{xy} and $d_{x^2-y^2}$ (for the easy axis) through $\vec{l}_z$ increases, with an aggregate effect of enhancing the MAE in the relaxed geometry.

The change of the easy axis can also be seen from the variation in the spin-orbit coupling matrix elements of the easy and the hard axis of magnetization. The spin-orbit matrix elements of the Co atom in the nonrelaxed and the relaxed Co-Pt chain reveal that the magnetization direction parallel to the surface is mostly determined by the spin-orbit coupling of $d_{3z^2-r^2}$ states with d_{xz} and d_{yz} ones, through $\vec{l}_x$. In the nonrelaxed geometry this firmly decides the spin-orbit coupling contribution to the ground state energy of the easy axis. The magnetization axis perpendicular to the surface is characterized by the SOC between d_{xy} and $d_{x^2-y^2}$ states by the $\vec{l}_z$ operator, in addition to the coupling already stated above. And these couplings play the main role here. Atomic relaxations decrease the interaction between $d_{3z^2-r^2}$ states with d_{xz} and d_{yz}, for the magnetization direction parallel to the surface. There is also an increase in the SOC between d_{xy} and $d_{x^2-y^2}$, which decreases the energy of the easy axis configuration for the relaxed geometry. From the variation stated above, the direction of the easy axis changes from parallel to the surface in nonrelaxed geometry to normal to the surface in relaxed geometry.

B. Effect of the electric field on the MAE

In this section we discuss the influence of the electric field on magnetic properties in the Co and the Co-Pt chains on the Pt(111) substrate. The strength of the electric field varying from -1.0 V/Å to 1.0 V/Å is used. The positive electric field is directed towards the surface, which supports the atomic chains (opposite to the z axis). Here we particularly analyze the tuning of the MAE ($E_{yz} = E_y - E_z$; $E_{xz} = E_x - E_z$) [Fig. 1(c)] of the Co and the Co-Pt chains on the Pt(111) surface by means of the electric field. The MAE of the Co chain and the Co-Pt chain as a function of the electric field is presented in Fig. 4. For both Co and Co-Pt chains the MAE shows linear-like dependence as a function of the electric field, and the MAE is enhanced when the strength of the electric field, directed outwards from the surface, increases.

The relative variation of the MAE (E_{yz}), when the electric field changes from 1.0 V/Å to -1.0 V/Å, is 67% and 57% for the Co chain and the Co-Pt chain, respectively, whereas E_{xz} increases by 34% and 39% in the same electric field range. The change of MAE in the absolute value is as large as 1.2 meV for the Co chain and 1.4 meV for the Co-Pt chain. The results discussed above suggest that for higher electric field one can switch the easy axis from out of plane to in plane along the chain (intermediate axis). The origin of the change in the MAE is related to the spatial redistribution of the electronic density in response to the electric field, and the corresponding changes of the density of states near the Fermi energy. Furthermore, the surface screening phenomena in ferromagnetic metals are found to be spin dependent.[70] Figure 5(a) shows the density of states for the p orbital (majority and minority) of the Co atom in different external electric fields. The majority

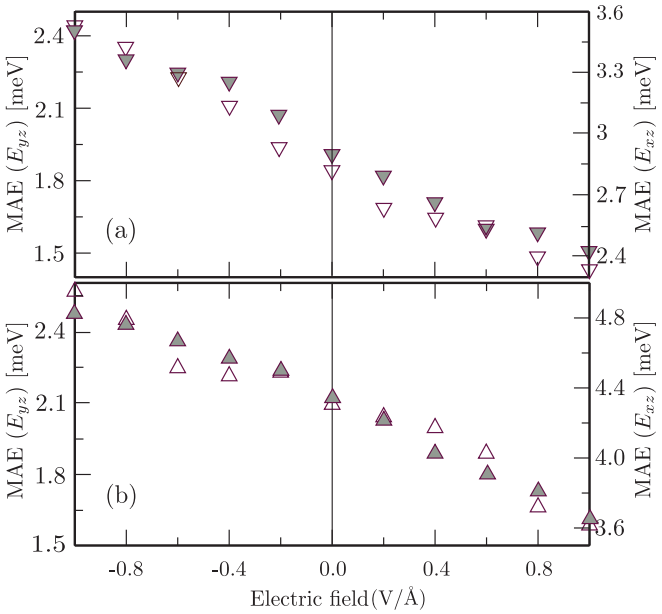

FIG. 4. (Color online) The effect of the electric field on the MAE of (a) the Co chains, and (b) the Co-Pt chain. In both cases [(a) and (b)] E_x, E_y, and E_z are hard, intermediate and easy axes, respectively. The shaded triangles represent E_{yz} and unshaded triangles are for E_{xz}.

and minority p electrons screen the electric field differently, in which the minority states show higher variation to the change of the electric field. This phenomenon has once more revealed the spin-polarized charge distribution on the vertical cross-sectional area above the Co-Pt atomic chain. Figure 6 shows the difference in the charge distribution when the system is exposed to the electric field of −0.8 V/Å and 0.8 V/Å $[\rho_{\uparrow(\downarrow)}(E=-0.8)-\rho_{\uparrow(\downarrow)}(E=0.8)]$ for both (a) the majority and (b) the minority spin channels. In this figure it is clearly seen that the effect of the external electric field on the minority states of Co is stronger than on the majority ones. This is associated with the screening by the delocalized p states [Fig. 5(a)], which in turn affects d states in the Co atom and alters the magnetic properties.

In Fig. 5(b) the orbital projected density of states for d orbitals of the Co atom (d_{yz} and $d_{3z^2-r^2}$) in the Co-Pt chain is presented, for the electric field of −0.8 V/Å, 0.0 V/Å, and 0.8 V/Å. No significant changes are observed in d_{xy}, d_{xz}, and $d_{x^2-y^2}$ states near the Fermi energy. Depending on the direction and the magnitude of the electric field, the density of states near the Fermi level changes. In particular, when the electric field is changed from 0.8 V/Å to −0.8 V/Å, the density of $d_{3z^2-r^2}$ states just below the Fermi energy decreases and the density of d_{yz} states above the Fermi energy rises.

As was mentioned in Sec. III A, in the Co-Pt chain the interactions of d_{xz} and d_{yz} with $d_{3z^2-r^2}$, through the $\vec{l}_x$ operator, are responsible for the hard-axis configuration. For the electric field of −0.8 V/Å there is significant decrease of $d_{3z^2-r^2}$ states just below the Fermi level, compared to these states at 0.8 V/Å. The coupling of d_{xz} and d_{yz} with $d_{3z^2-r^2}$ for the field −0.8 V/Å also decreases, compared to the couplings for the field 0.8 V/Å. This increases the energy of the hard-axis configuration. Recalling the second-order perturbation Eq. (1), one can see that the operator $\vec{l}_x$ couples the occupied and

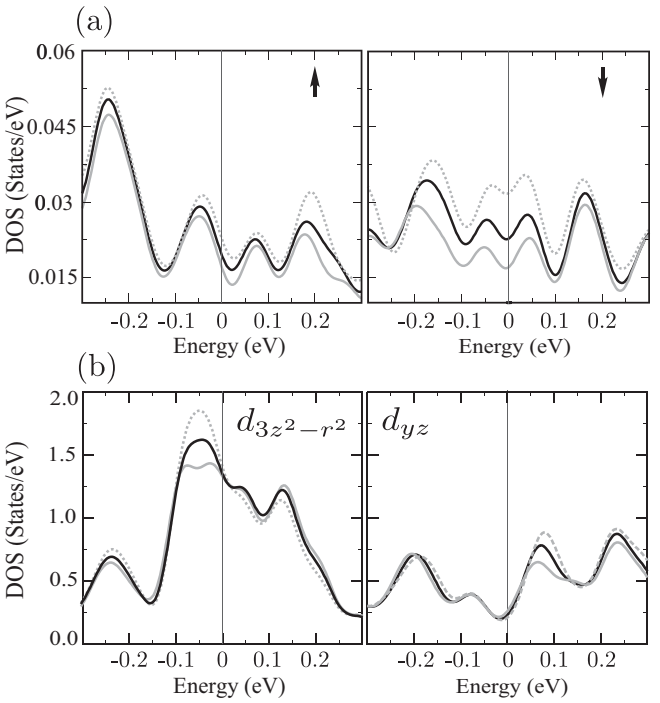

FIG. 5. (a) The density for p states of the Co atom in the Co-Pt chain for spin up and spin down is presented. (b) Orbital-projected d LDOS of the Co atom in Co-Pt mixed chain for minority states of d_{yz}, $d_{3z^2-r^2}$. The gray line, full line, and dashed line represent density of states at −0.8 V/Å, 0.0 V/Å, and 0.8 V/Å electric fields, respectively.

unoccupied states of d_{xz} and d_{yz} with $d_{3z^2-r^2}$, and the coupling is stronger for 0.8 V/Å than −0.8 V/Å. This has an effect of decreasing the second term in the numerator at −0.8 V/Å, which obviously gives higher MAE. Displacement of the atomic chains due to the electric field, i.e., 0.6 mÅ per 1 V/Å in the Co-Pt chain, is negligibly small.

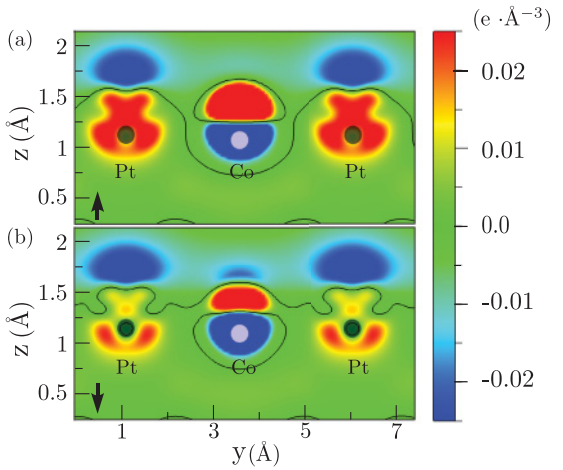

FIG. 6. (Color) The difference in the charge distribution at −0.8 V/Å and 0.8 V/Å plotted over vertical section which crosses the atomic chains, for (a) the majority and (b) the minority states. The contour lines represent zero charge difference. The dimensions z and y measure the vertical and the horizontal distances of the cross-section.

IV. CONCLUSION

Based on the *ab initio* approach, we have calculated the MAE and the magnetic easy axis of the pure Co chains and the mixed Co-Pt chains supported on the Pt(111) surface. The MAE in the Co-Pt chain increases by more than one third, compared to the Co chain. The relaxed geometry of the Co chain and the Co-Pt chain has an easy axis normal to the surface. We have demonstrated the tuning of the MAE by means of the electric field. In both Co and Co-Pt chains the MAE increases as the electric field directed outward from the surface increases. It is shown that the spin-dependent screening of the electric field at chains plays a dominant role in their magnetic properties.

*stepanyu@mpi-halle.mpg.de

[1] E. Y. Tsymbal, Nat. Mater. **11**, 12 (2012).
[2] G. A. Prinz, Science **282**, 1660 (1998).
[3] H. Ohno, D. Chiba, F. Matsukura, T. Omlya, E. Abe, T. Dletl, Y. Ohno, and K. Ohtanal, Nature (London) **408**, 944 (2000).
[4] N. A. Spaldin and M. Feibig, Science **309**, 391 (2005).
[5] M. Fiebig, J. Phys. D **38**, R123 (2005).
[6] S. Sahoo, S. Polisetty, C. G. Duan, S. S. Jaswal, E. Y. Tsymbal, and C. Binek, Phys. Rev. B **76**, 092108 (2007).
[7] T. Lonkai, D. G. Tomuta, U. Amann, J. Ihringer, R. W. Hendrikx, D. M. Tobbens, and J. A. Mydosh, Phys. Rev. B **69**, 134108 (2004).
[8] T. Klumra, T. Goto, H. Shintani, K. Ishizaka, T. Arima, and Y. Tokura, Nature (London) **426**, 55 (2003).
[9] T. Lottermoser, T. Lonkal, U. Amann, D. Hohlweln, J. Ihringer, and M. Fiebig, Nature (London) **430**, 541 (2004).
[10] S. M. Wu, S. H. A. Cybart, P. Yu, M. D. Rossell, J. X. Zhang, R. Ramesh, and R. C. Dynes, Nat. Mater. **9**, 756 (2010).
[11] R. Ramesh and N. Hill, Nature (London) **6**, 21 (2007).
[12] D. Chiba, M. Sawicki, Y. Nakatani, F. Matsukura, and H. Ohno, Nature (London) **455**, 517 (2008).
[13] Y. Yamada, K. Ueno, T. Fukumura, H. T. Yuan, H. Shimotani, Y. Iwasa, L. Gu, S. Tsukumito, Y. Ikuhara, and M. Kawastal, Science **332**, 1065 (2011).
[14] M. Weisheit, S. Fahler, A. Marty, Y. Souche, C. Poinsignon, and D. Givord, Science **315**, 349 (2007).
[15] P. Gambardella, S. Rusponi, M. Veronese, S. S. Dhesi, C. Grazioli, A. Dallmeyer, I. Cabiria, R. Zeller, P. H. Dederichs, K. Kern, C. Carbone, and H. Brune, Science **300**, 1130 (2003).
[16] P. Błoński and J. Hafner, J. Phys.: Condens. Matter **21**, 426001 (2009).
[17] S. Baud, C. Ramseyer, G. Bihlmayer, and S. Blügel, Phys. Rev. B **73**, 104427 (2006).
[18] P. Gambardella, A. Dallmeyer, K. Maiti, M. C. Malagoli, S. Rusponi, P. Ohresser, W. Eberhardt, C. Carbone, and K. Kern, Phys. Rev. Lett. **93**, 077203 (2004).
[19] S. Rusponi, T. Cren, N. Weiss, M. Epple, P. Buluschek, L. Claude, and H. Brune, Nat. Mater. **2**, 546 (2003).
[20] B. Lazarovits, L. Szunyogh, and P. Weinberger, Phys. Rev. B **67**, 024415 (2003).
[21] P. Gambardella, A. Dallmeyer, K. Maiti, M. C. Malagoli, W. Eberhardt, K. Kern, and C. Carbone, Nature (London) **416**, 301 (2002).
[22] B. Nonas, I. Cabria, R. Zeller, P. H. Dederichs, T. Huhne, and H. Ebert, Phys. Rev. Lett. **86**, 2146 (2001).
[23] Š. Pick, P. A. Ignatiev, A. L. Klavsyuk, W. Hergert, V. S. Stepanyuk, and P. Bruno, J. Phys.: Condens. Matter **19**, 446001 (2007).
[24] T. Balashov, T. Schuh, A. F. Takacs, A. Ernst, S. Ostanin, J. Henk, I. Mertig, P. Bruno, T. Miyamachi, S. Suga, and W. Wulfhekel, Phys. Rev. Lett. **102**, 257203 (2009).
[25] M. Ozerov, A. A. Zvyagin, E. Čižmár, J. Wosnitza, R. Feyerherm, F. Xiao, C. P. Landee, and S. A. Zvyagin, Phys. Rev. B **82**, 014416 (2010).
[26] N. Nilius, T. M. Wallis, and W. Ho, Science **297**, 1853 (2002).
[27] K. F. Braun and K. H. Rieder, Phys. Rev. Lett. **88**, 096801 (2002).
[28] S. Fölsch, P. Hyldgaard, R. Koch, and K. H. Ploog, Phys. Rev. Lett. **92**, 056803 (2004).
[29] J. Lagoute, C. Nacci, and S. Fölsch, Phys. Rev. Lett. **98**, 146804 (2007).
[30] N. N. Negulyaev, V. S. Stepanyuk, L. Niebergall, P. Bruno, W. Hergert, J. Repp, K. H. Rieder, and G. Meyer, Phys. Rev. Lett. **101**, 226601 (2008).
[31] A. A. Khajetoorians, J. Wiebe, B. Chilian, and R. Wiesendanger, Science **332**, 1062 (2011).
[32] H. Roder, E. Hahn, H. Brune, J. P. Bucher, and K. Kern, Nature (London) **366**, 141 (1993).
[33] A. A. Stekolnikov, F. Bechstedt, M. Wisniewski, J. Schäfer, and R. Claessen, Phys. Rev. Lett. **100**, 196101 (2008).
[34] O. V. Stepanyuk, N. N. Negulyaev, P. A. Ignatiev, M. Przybylski, W. Hergert, A. M. Saletsky, and J. Kirschner, Phys. Rev. B **79**, 155410 (2009).
[35] D. H. Wei, C. L. Gao, Kh. Zakeri, and M. Przybylski, Phys. Rev. Lett. **103**, 225504 (2009).
[36] T. Maruyama, Y. Shiota, T. Nozaki, K. Ohta, N. Toda, M. Mizuguchi, A. A. Tulapurkar, T. Shinjo, M. Shiraishi, S. Mizukamil, Y. Ando, and Y. Suzuki, Nat. Nanotechnol. **4**, 158 (2009).
[37] K. Nakamura, R. Shimabukuro, Y. Fujiwara, T. Akiyama, T. Ito, and A. J. Freeman, Phys. Rev. Lett. **102**, 187201 (2009).
[38] M. C. Troparevsky, K. Zhao, D. Xiao, Z. Zhang, and A. G. Eguiluz, Nano Lett. **9**, 12 (2009).
[39] S. J. Gamble, M. H. Burkhardt, A. Kashuba, R. Allenspach, S. S. P. Parkin, H. C. Siegmann, and J. Stohr, Phys. Rev. Lett. **102**, 217201 (2009).
[40] W. G. Wang, M. Li, S. Hageman, and C. L. Chien, Nat. Mater. **11**, 64 (2012).
[41] Y. Shiota, T. Takayuki, F. Bonell, S. Murakami, T. Shinjo, and Y. Suzuki, Nat. Mater. **11**, 39 (2012).
[42] K. Nakamura, R. Shimabukuro, T. Akiyama, T. Ito, and A. J. Freeman, Phys. Rev. B **80**, 172402 (2009).
[43] Y. Sun, J. D. Burton, and E. Y. Tsymbal, Phys. Rev. B **81**, 064413 (2010).
[44] S. Haraguchi, M. Tsujikawa, and J. Gotou, J. Phys. D **44**, 064005 (2011).
[45] M. Tsujikawa and T. Oda, Phys. Rev. Lett. **102**, 247203 (2009).
[46] C. G. Duan, J. P. Velev, R. F. Sabirianov, Z. Zhu, J. Chu, S. S. Jaswal, and E. Y. Tsymbal, Phys. Rev. Lett. **101**, 137201 (2008).
[47] N. N. Negulyaev, V. S. Stepanyuk, W. Hergert, and J. Kirschner, Phys. Rev. Lett. **106**, 037202 (2011).

[48]L. Gerhard, T. K. Yamada, T. Balashov, A. F. Takács, R. J. H. Wesselink, M. Däne, M. Fechner, S. Ostanin, A. Ernst, I. Mertig, and W. Wulfhekel, Nat. Nanotechnol. **5**, 792 (2010).
[49]H. Zhang, M. Richter, K. Koepernik, I. Opahle, F. Tasnádi, and H. Eschrig, New J. Phys. **11**, 043007 (2009).
[50]M. Tsujikawa and T. Oda, J. Phys. D **38**, R123 (2005).
[51]P. A. Ignatiev and V. S. Stepanyuk, Phys. Rev. B **84**, 075421 (2011).
[52]A. Mosca Conte, S. Fabris, and S. Baroni, Phys. Rev. B **78**, 014416 (2008).
[53]P. E. Blöchl, Phys. Rev. B **50**, 17953 (1994).
[54]G. Kresse and D. Joubert, Phys. Rev. B **59**, 1758 (1999).
[55]G. Kresse and J. Hafner, Phys. Rev. B **47**, 558 (1993).
[56]G. Kresse and J. Furthmüller, Phys. Rev. B **54**, 11169 (1996).
[57]D. M. Ceperley and B. J. Alder, Phys. Rev. Lett. **45**, 566 (1980).
[58]J. P. Perdew, K. Burke, and M. Ernzerhof, Phys. Rev. Lett. **77**, 3865 (1996).
[59]F. Birch, Phys. Rev. **71**, 809 (1947).
[60]J. Neugebauer and M. Scheffler, Phys. Rev. B **46**, 16067 (1992).
[61]We have checked the convergence of our results with respect to the number of Pt layers. The easy axis is unchanged; however, similarly to Ref. 63, the MAE exhibits small oscillations with the amplitude of 0.3 meV for the number of Pt layers less than 6. This does not affect the main results of the paper. We have also checked calculations of the MAE for larger numbers of k points, for example $5 \times 10 \times 1$, and found only minor changes.
[62]For the unrelaxed geometry the interaction between Pt and Co is still too weak to enhance the MAE.
[63]O. Šipr, S. Bornemann, J. Minár, and H. Ebert, Phys. Rev. B **82**, 174414 (2010).
[64]P. Giannozzi *et al.*, J. Phys.: Condens. Matter **21**, 395502 (2009).
[65]P. Bruno, Phys. Rev. B **39**, 865 (1989).
[66]G. Autès, C. Barreteau, D. Spanjaard, and M. Desjonquères, J. Phys.: Condens. Matter **18**, 6785 (2009).
[67]A. B. Shick, F. Máca, and A. I. Lichtenstein, Phys. Rev. B **79**, 172409 (2009).
[68]D. S. Wang, R. Wu, and A. J. Freeman, Phys. Rev. B **47**, 14932 (1993).
[69]G. Kresse and O. Lebacq, VASP manual [http://cms.mpi.univie.ac.at/vasp/].
[70]S. Zhang, Phys. Rev. Lett. **83**, 640 (1999).